Lab on a Chip

Cite this: *Lab Chip*, 2012, **12**, 802

www.rsc.org/loc

PAPER

High throughput production of single core double emulsions in a parallelized microfluidic device

Mark B. Romanowsky,[a] Adam R. Abate,[b] Assaf Rotem,[a] Christian Holtze[c] and David A. Weitz[a]

Received 25th October 2011, Accepted 19th December 2011
DOI: 10.1039/c2lc21033a

Double emulsions are useful templates for microcapsules and complex particles, but no method yet exists for making double emulsions with both high uniformity and high throughput. We present a parallel numbering-up design for microfluidic double emulsion devices, which combines the excellent control of microfluidics with throughput suitable for mass production. We demonstrate the design with devices incorporating up to 15 dropmaker units in a two-dimensional or three-dimensional array, producing single-core double emulsion drops at rates over 1 kg day^{-1} and with diameter variation less than 6%. This design provides a route to integrating hundreds of dropmakers or more in a single chip, facilitating industrial-scale production rates of many tons per year.

Double emulsions (drops within drops) are versatile templates for production of many different kinds of microcapsules and functional particles.[1,2] Potential applications range from the encapsulation and release of drugs or other molecules[3–5] to production of Janus particles for use as surfactants or self-assembling materials.[6,7] Simple emulsions can be produced in large quantity and with reasonable uniformity by high-shear mixers or high-pressure homogenizers; but using these machines to re-emulsify an emulsion usually produces an uncontrollable mix of double emulsions with greatly varying size and numbers of inner drops, plus large losses of the core phase into the continuous phase, unless the visco-elasticity of the fluids is carefully tuned.[8,9] These problems are serious limitations for many applications of double emulsions: high polydispersity lessens the ability to control the release profile of encapsulated drugs, and yields of the desired capsule or particle morphology can be very low. A major obstacle for these applications is the lack of any suitable method for making double emulsions sufficiently monodisperse while also in sufficient quantities to be useful. In contrast to bulk emulsification methods, microfluidic devices afford unrivaled fine control over the double emulsification process, capable of producing drops with very thin shells, nearly perfect loading efficiency, and low polydispersity. However, this is typically at the cost of limited throughput of millilitres per hour or less.[10,11] Increasing throughput merely by using multiple separate devices is not feasible, because each device needs a set of pumps to supply fluids; if more than a handful of devices are used, this method rapidly becomes both expensive and logistically difficult. Therefore, an attractive strategy for increasing throughput is to integrate many copies of a microfluidic device in a single chip, and drive the assembly with a single set of pumps. Parallelized microfluidic devices of this kind have been demonstrated for producing larger quantities of simple emulsions,[12–15] but to date such devices have been unable to produce double emulsions, and a viable route to scalability has not been demonstrated. A device combining the excellent precision of microfluidics with the industrial-scale productivity of bulk emulsifiers is needed before double emulsions can truly emerge as a useable template for microcapsules and complex particles.

In this paper, we present a parallel numbering-up design for microfluidic double emulsification devices, which increases throughput greatly while maintaining good product uniformity. We demonstrate devices integrating up to 15 dropmaker units, producing single-core double emulsion drops at rates over 1 kg day^{-1} with inner and outer diameter variation below 6%. We repeat the basic dropmaker units in both a two-dimensional and a three-dimensional array, and connect them using a three-dimensional network of much larger distribution and collection channels. By making the distribution channels with much lower flow resistance than the dropmaker units, we apportion the input fluids evenly to all dropmakers and obtain drops with a narrow size distribution. Our design follows simple and favorable scaling rules, and provides a route to increase throughput further yet. By integrating hundreds of dropmaker units or even more, we anticipate a device occupying one litre of space that produces uniform double emulsion at more than one litre per hour, or nearly nine tons per year. Such a device could be the basis for industrial-scale production rates of many tons per year.

Our parallelized integrated chip is made of many copies of a basic dropmaker unit. This unit comprises two consecutive junctions in which the channel width and height are both

[a]*School of Engineering and Applied Sciences and Department of Physics, Harvard University, Cambridge, USA*
[b]*Department of Bioengineering and Therapeutic Sciences, Schools of Medicine and Pharmacy, University of California, San Francisco, USA*
[c]*BASF SE, Ludwigshafen, Germany*

increased after the second junction, as shown in the schematic in Fig. 1a. This geometry allows the shell phase fluid to be hydrodynamically focused by the continuous phase, and thus kept away from the channel surfaces, which it could otherwise wet and adhere to.[16,17] By graduating the channel in this way, we avoid having to pattern channel wettability, as is normally required to make double emulsions.[6,16] Additionally, both junctions are swept crosses in which the enveloping phase channels meet the dispersed phase channel at an angle, as shown in Fig. 1a, b. This angled junction avoids the stagnation points that would be present at the height step in an orthogonal junction, and this improves the stability of the hydrodynamic focusing. With the height graduation as well as the angled junction, we are able to reliably turn on and operate the dropmaker without the shell phase wetting the channel surfaces. We run the devices in the "one-step" double emulsification mode,[16] which avoids the difficulty of matching the frequencies of different dropmaker junctions and thus improves drop uniformity.

To create a parallel integrated chip with higher throughput, we lay out several copies of our microfluidic dropmaker unit in a horizontal array, and join each unit vertically to much larger distribution and collection channels using vertical through-holes, as shown in Fig. 1c, d. The sizes of the distribution channels and collection channels are determined by our requirement that all fluids be apportioned equally between all the dropmaker units, so that each dropmaker will produce the same size drops. The channels must be large enough that the flow resistance R_c along the channels, from one dropmaker to its neighbor, is negligible compared to the flow resistance R_u through a dropmaker unit, from its inlet to its outlet. If R_c is much less than R_u, then the corresponding pressure drops have the same relation, and each unit will receive an equal flow rate of each fluid, accurate to order (R_c/R_u). To calculate the required channel dimensions, we consider a ladder-like network of channels, in which the lengthwise channels correspond to our distribution and collection channels, and the cross-wise "rung" channels correspond to our dropmaker units, as illustrated in Fig. 2. We determine the pressures and flows through the various channels using lumped-element analysis. We calculate the flow resistances R_c and R_u using the equation for laminar flow through a rectangular pipe:[18]

$$R = 12(\mu L/wh^3)(1 - 0.63(h/w))^{-1}$$

in which μ is the fluid viscosity, L, w, and h are the channel length, width, and height with $w > h$, and we neglect terms of higher order in (h/w). This approximation is within 14% of the exact calculation for $h = w$, and rapidly becomes more exact as (h/w) increases. Using these resistances, we determine the flows and pressures through the network with a system of linear equations. In a ladder with two rungs, the ratio of flow rates through the two dropmaker units is

$$Q_1/Q_2 = 1 + 2(R_c/R_u).$$

In a ladder with more rungs, the same general result holds: the difference in flow rates between neighboring dropmaker units is order (R_c/R_u), and therefore the maximum difference in flow rates between any two units is order $N(R_c/R_u)$. Our design criterion is to make the distribution channels large enough that $2N(R_c/R_u) < 0.01$. Using these distribution channels, we supply the core, shell, and continuous phase fluids to a single set of inlets, the fluids are divided evenly among the dropmaker units, each dropmaker produces a very narrow distribution of double emulsion drops, and finally the drops are delivered through a collection channel to a common outlet.

To increase the packing density of dropmaker units, we can parallelize in all three dimensions, using a three-stage nested design. In our first stage of parallelization, we lay out several dropmaker units in a line, and join them using a first, primary distribution layer directly above the dropmaker layer. In this way, we reduce all the units in the line to a single set of inlets and outlets. In our second stage of parallelization, we lay out several dropmaker units in a rectangular array. Each line of units is joined by its own set of distribution and collection channels in a common primary distribution layer. We then join all these lines

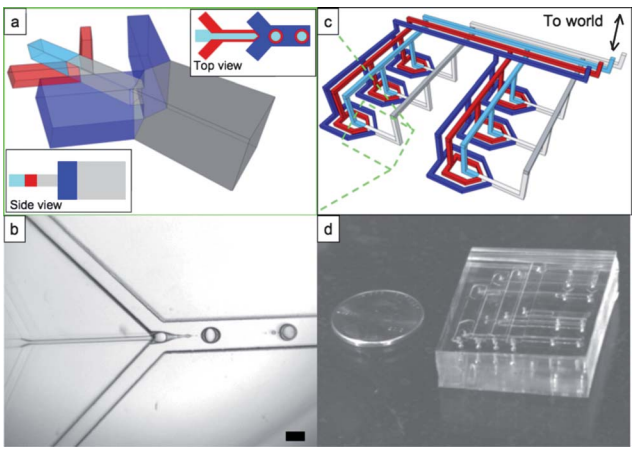

Fig. 1 (a) Schematic of a microfluidic double emulsion-maker unit, not to scale. Insets: top view and side view schematics showing angled junctions and height step. (b) Micrograph of a unit producing double emulsion drops; the scale bar denotes 100 μm. (c) Schematic of a parallelized double emulsion chip, comprising rows of microfluidic double emulsifier units that are connected through vertical through-holes to a layer of much larger distribution/collection channels, with each integrated row connected to another layer of yet larger distribution/collection channels. Channels marked light blue carry the core fluid, red the shell fluid, dark blue the continuous phase fluid, and gray the double emulsion product. (d) Photograph of an integrated chip; the coin (a US penny) is 19 mm across.

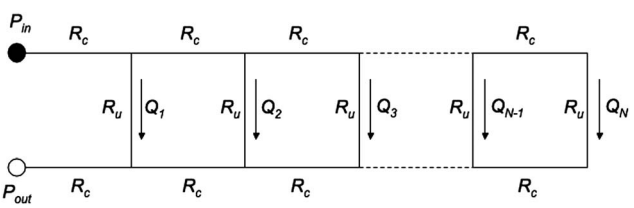

Fig. 2 A ladder-like network of channels, used as a model for our parallelized dropmaker devices. Lengthwise elements are the distribution and collection channels, with flow resistance R_c per segment; cross-wise elements are the dropmaker units, with flow resistance R_u. Dropmaker unit i passes fluid at a flow rate Q_i. Because we design the channels such that $R_c \ll R_u$, all the flows Q_i are equal to order $N(R_c/R_u)$.

together with a secondary distribution layer of yet larger distribution and collection channels. We design the secondary distribution layer using lumped-element analysis again: a row of N dropmaker units, coupled by a primary distribution layer, can be considered a single element having flow resistance approximately R_u/N. Then we require that the secondary distribution layer, coupling M such rows, have flow resistance R_{c2} satisfying $2M(R_{c2}/(R_u/N)) < 0.01$. This ensures that each linear array receives an equal amount of each fluid and produces similar drops. In this way, we integrate a two-dimensional, area-filling array of dropmakers using two distribution layers. In our final stage of parallelization, we laminate together multiple xy-planar arrays of dropmaker units, each plane having its own primary and secondary distribution layers, and join the planes with vertical (z-axis) tertiary distribution channels. We once more apply the same lumped-element method to ensure that each planar array receives equal amounts of fluid and produces similar drops. In this way, we integrate a three-dimensional, volume-filling cubic array of dropmaker units, linked by a three-dimensional network of distribution and collection channels.

For ease of prototyping, we make all our devices from PDMS using soft lithography techniques. Our fabrication process begins with well-known replica molding;[19] however, because our dropmaker unit includes height steps both upwards and downwards at the second junction, it cannot be molded in a single step from a single master. We therefore design the dropmaker in top and bottom halves, and mold replicas of the halves on different masters. The dropmaker channels are 50 μm wide and 50 μm high upstream of the second junction, but downstream the channels are 190 μm wide and 150 μm high, with both the channel floor lowered and ceiling raised by 50 μm. We make inlet and outlet holes to each dropmaker unit using a biopsy punch. We align the two halves using a "mortise and tenon" method,[20] and plasma bond them together. We then plasma bond the dropmaker layer to the distribution layers. After assembling the device, we hydrophobize all channel surfaces by injecting Aquapel (PPG Industries) through the device, blowing it out with air, and finally baking dry in an oven at 65 °C.

To demonstrate the devices, we choose working fluids that form double emulsions at moderate flow rates. Our double emulsions have cores of sodium alginate in water at 0.25%wt, and shells of 1-octanol with 0.5%wt ABIL EM 90 surfactant (Evonik Industries), and are dispersed in a continuous phase of 3%wt poly(vinyl alcohol) in water. Double emulsions can also be made using other oils, such as perfluorocarbons instead of octanol, or other surfactants, such as sodium dodecyl sulfate instead of poly(vinyl alcohol), but in these cases the hydrodynamic focusing at the second junction can require inconveniently high continuous phase flow. The sodium alginate increases the viscosity of the core fluid, so that we can use our dropmakers in the single-step regime with a thicker shell than would be possible with a pure water core. This allows us to make reliable optical measurements of shell thickness, which we use to validate our devices. Such a viscous core fluid also results in the production of some very small satellite drops, which we disregard in our analysis.

We normally drive each phase with a syringe pump. However, in devices with large numbers of dropmakers, we instead use a peristaltic pump to supply the continuous phase at the required high flow rates. Remarkably, the pulsation of the peristaltic pump causes only a modest rise in the polydispersity of the drops. We attribute this to the elastic compliance of the whole PDMS system, which damps out the pulsation.

To validate our devices, we image many double emulsion drops with a digital video microscope, apply image analysis software to determine the core and shell size of each drop, and then compute statistics on the distribution. We first measure the distribution from a single, non-arrayed dropmaker unit.

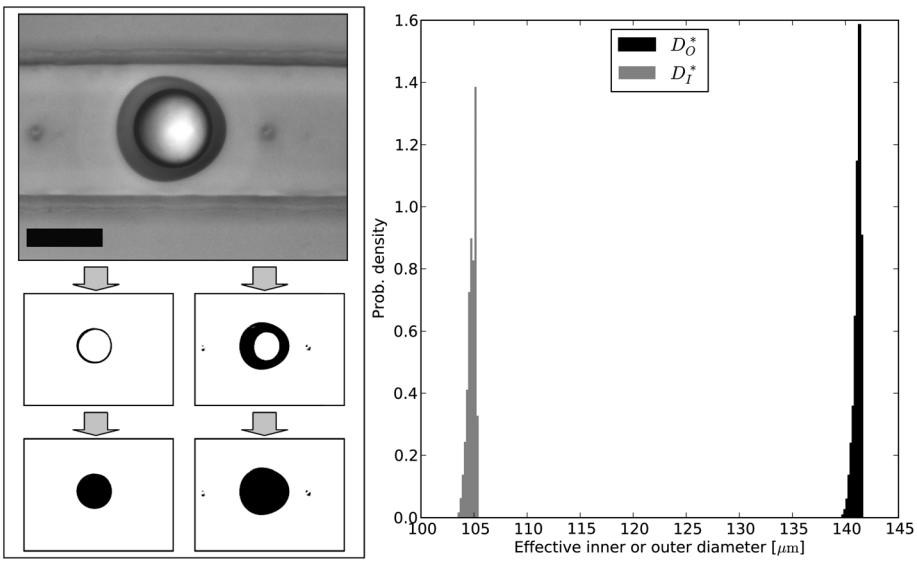

Fig. 3 (Left) Typical micrograph used for drop sizing, and the processing steps used to determine core and total areas. Scale bar indicates 100 μm. (Right) Distribution of drop sizes from an individual dropmaker unit. Size is determined as the effective inner and outer diameters D_I^* and D_O^*, which are the diameters of circles having the same areas as the images of the core drop and whole double emulsion drop, respectively. Sample size = 1200 drops. Inner diameter CV = 0.35%, outer diameter CV = 0.23%.

We image over 1000 drops from the dropmaker, so that we can accurately measure the very narrow size distribution. Images are collected using a 20X Mitutoyo long-working-distance objective and recorded by a Sony XCD-V60 camera. Drops flow past the field of view fast enough that no individual drop appears in more than one frame of video. We use our own LabVIEW program to analyze the video images after capture. For each movie, our program finds an averaged background by averaging all of its frames, pixel by pixel. Each frame in the movie is normalized by dividing it by the background, pixel by pixel. Each normalized frame is then thresholded to find the very dark "rim" around the drop core that is present when the drop is properly focused, and thresholded independently to find the moderately dark shell; this process is shown for a typical drop image in Fig. 3(left). We determine the areas of the core and shell regions of the drop image; with about 10^4 pixels typically in each region, pixel noise is low. Drop cross-sections are distorted from circular by viscous drag as they flow in the microchannels. Thus, for each drop image, we calculate effective inner and outer diameters D_I^* and D_O^*, which are the diameters of circles having the same core area and total area (respectively) as the drop image. Our dropmaker produces extremely uniform double emulsions, showing coefficients of variation (or CV, defined as standard deviation divided by mean) of D_I^* and D_O^* below 0.5%; a typical histogram of drop sizes is shown in Fig. 3 (right).

We validate our parallelized devices in the same way. We first test a linear array of five dropmaker units, joined by a primary distribution layer. We image over 1000 drops from each unit, and determine the inner and outer diameters. Each dropmaker makes extremely uniform double emulsions, with a very peaked diameter distribution, and the peaks of all the dropmakers are tightly clustered, as shown in Fig. 4 (top). The parallelized device overall produces drops with a narrow distribution, with CV of D_I^* and D_O^* equal to 4.4% and 1.3%, respectively. The spread in the five peaks is close to what is allowed by the design criteria for our distribution layer, which keeps the flow rates to each unit equal to within about 1%.

We demonstrate simultaneous high throughput and narrow size distribution using a 3 × 5 planar array of 15 dropmaker units, with primary and secondary distribution layers. This device is small, occupying only 25 cm^3. We supply the core aqueous phase at 24 mL h^{-1} and the shell octanol phase at 30 mL h^{-1} using syringe pumps. We supply the continuous aqueous phase at 215 mL h^{-1}, but in this case using a peristaltic pump (Minipuls 3, Gilson Inc.) to supply such a high flow rate. Run continuously at this rate for a full day, the device would produce 1.5 kg of double emulsion drops, dispersed in 5.2 kg of continuous phase. All 15 dropmaker units produce single-core double emulsion drops of the same general size, as shown in the micrographs in Fig. 4. As a more quantitative measure of the drop size distribution, we capture and analyze 13590 drop images, sampled for equal times from 8 of the 15 dropmakers. We obtain a narrow distribution with inner and outer diameter CV of 5.7% and 4.1%, respectively, as shown in Fig. 4(middle). This polydispersity is due in part to the peak shifting of one dropmaker relative to another, as observed in our linear array, but also due in part to peak broadening caused by the pulsation of the peristaltic pump, which periodically modulates the overall drop sizes. Each individual dropmaker unit has CV about 3% when we use the peristaltic pump, as compared to CV less than 0.5% when we use syringe pumps. This broadening, combined with the few-percent peak shifting allowed by our distribution layers, accounts for the observed CV in the 3 × 5 array. We expect that both of these contributions to the polydispersity will remain controlled as more and more dropmakers are arrayed together. For even better uniformity, the device could be driven completely by non-pulsating fluid sources such as overpressure-regulated fluid reservoirs.

In principle, a parallel three-dimensional array of dropmaker units will work similarly to the one- and two-dimensional arrays, but to make such a device reliably may exceed the limits of soft lithographic fabrication. Nonetheless, to illustrate the progression from individual units to 3-d arrays, we make a series of devices with 1, 2, 4(=2 × 2), and 8(=2 × 2 × 2) dropmaker units.

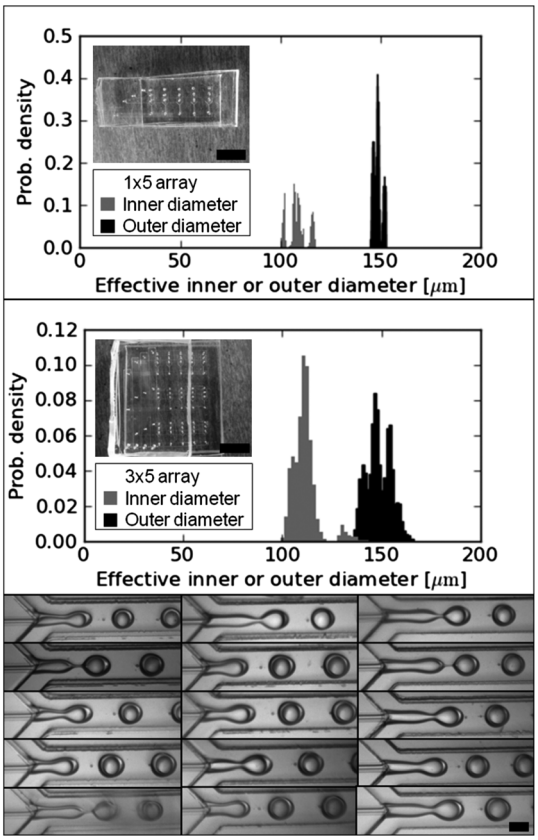

Fig. 4 (Top) Distribution of drop sizes for a 5-unit (1 × 5) array, pictured in inset; scale bar denotes 1 cm. Production rate is 10 mL h^{-1} dispersed phases (4 mL h^{-1} core + 6 mL h^{-1} shell). Size is the effective inner and outer diameters D_I^* and D_O^*, which are the diameters of circles having equal areas to the images of the core drop and whole double emulsion drop, respectively. Sample size = 7796, sampled for equal times from each dropmaker unit. Inner diameter CV = 4.4%, outer diameter CV = 1.3%. (Middle) Distribution of drop sizes for a 15-unit (3 × 5) array, pictured in inset; scale bar denotes 1 cm. Production rate is 54 mL h^{-1} dispersed phases (24 mL h^{-1} core + 30 mL h^{-1} shell). Sample size = 13590, sampled for equal times from 8 of the 15 dropmaker units. Inner diameter CV = 5.7%, outer diameter CV = 4.1%. (Bottom) Micrographs of all 15 dropmaking units in the 3 × 5 array, producing single-core double emulsions. The unit in the lower right corner is closest to the inlets and outlets. Scale bar indicates 100 μm.

Each device in the series produces uniform, single-core double emulsion drops, and the throughput of each device is proportional to the number of dropmaker units, as shown in Fig. 5. The devices are again small: the 2 × 2 × 2 array, which has the greatest proportion of auxiliary plumbing, occupies only 25 cm^3. The 2 × 2 × 2 device comprises eight laminated layers of PDMS, all of which must be precisely aligned to accommodate long vertical through-holes. This alignment is difficult and not fully reproducible in a soft elastic material like PDMS, but could be easier in a more rigid material such as glass or polycarbonate. Like our other devices, the example 2 × 2 × 2 device makes generally uniform drops, as shown in Fig. 5(right). Unfortunately, a piece of debris caused one junction to fail; however, this highlights a useful feature of our design: because we have designed a negligible coupling between adjacent dropmaker units, the failure of this dropmaker unit does not affect the performance of the other seven units in the device.

Our design can accommodate much larger numbers of dropmaker units with only simple and straightforward changes. Our distribution system design displays a favorable scaling in the number of dropmaker units. If we pack more dropmakers along a linear array without changing the distribution channels, increasing N to αN, then the distance between neighboring dropmakers is divided by α, the flow resistance per segment of the distribution channel decreases from R_c to R_c/α, and the figure of merit $2N(R_c/R_u)$ is unchanged. Similarly, in 2- or 3-dimensional arrays, the figure of merit is $2MN(R_{c2}/R_u)$ for the secondary distribution channels, and $2LMN(R_{c3}/R_u)$ for the tertiary distribution channels. If packing density is increased by a factor α along every dimension, then to keep the figures of merit constant the heights of the secondary and tertiary channels must be increased by only $\alpha^{1/3}$ and $\alpha^{2/3}$, respectively. Our design can therefore be followed with only small modifications until the packing density is so great that channels begin to overlap. We estimate that up to a 4 × 16 array could be fit on a 3-inch wafer without overlap. A further reduction in the dropmaker footprint, which is mostly due to inlet and outlet channels and not to the dropmaker junctions themselves, could again double the packing density in each dimension, to over 250 dropmakers per planar replica. With multiple planes laminated and integrated together, some 1000 or more dropmaker units could fit in a single device occupying less than 1000 cm^3. Extrapolating linearly, we estimate that such a device could produce over 30 tons per year of double emulsion droplets. If even greater production rates are required, the dropmaker design could be further optimized to increase throughput per unit.

We have demonstrated our parallelized microfluidic design by making double emulsions of water/octanol/water, but we

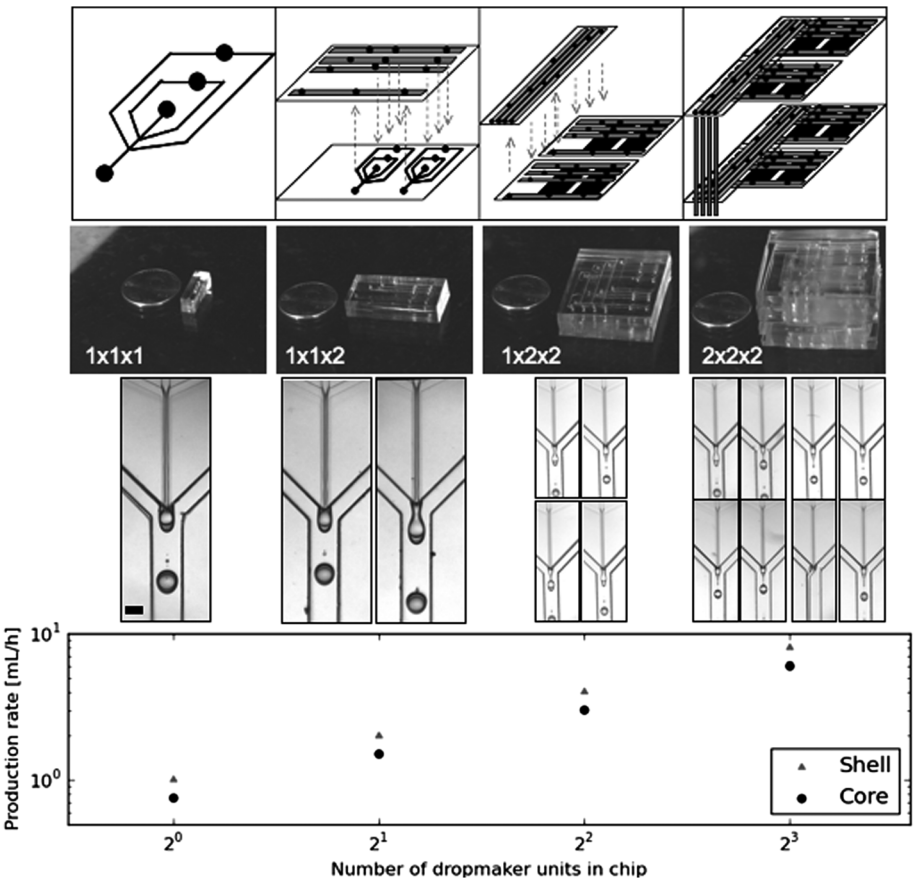

Fig. 5 Double emulsification chips can comprise (from left to right) 0-, 1-, 2-, and 3-dimensional tilings of microfluidic dropmaker units. (Top) Schematic sketches of the dropmaker units, with laminated distribution and collection channels, tiled in 0 to 3 dimensions. (Upper middle) Photographs of the devices; the coin (a US penny) is 19 mm across. (Lower middle) Micrographs of dropmaker units producing highly uniform single-core double emulsion drops. Scale bar indicates 100 μm. (Bottom) The production rate of double emulsions is proportional to the number of dropmaking units in the device.

emphasize that the design is suitable for a variety of uses. Very similar devices will have direct applications making microcapsules for the controlled release of active molecules, as well as double-emulsion-templated complex particles. Moreover, our distribution system is very general. It could be adapted easily for high-throughput simple emulsification, or for micro-spray-drying devices used to form rapidly soluble nm-scale drug particles.[21] Our device provides a model for parallelized, high-throughput versions of any continuous-flow microfluidic device, and we expect it will work up to production rates of tons per year and beyond. This shows a potential scale-up route for the microfluidic manufacture of precision particles and capsules at the commodity scale.

Acknowledgements

This work was supported by BASF SE, the NSF (grant DMR-1006546), and the MRSEC (grant DMR-082084). This work was performed in part at the Center for Nanoscale Systems (CNS), a member of the National Nanotechnology Infrastructure Network (NNIN), which is supported by the National Science Foundation under NSF award no. ECS-0335765. CNS is part of Harvard University.

References

1 Rhutesh K. Shah, Ho Cheung Shum, Amy C. Rowat, Daeyeon Lee, Jeremy J. Agresti, Andrew S. Utada, Liang-Yin Chu, Jin-Woong Kim, Alberto Fernandez-Nieves, Carlos J. Martinez and David A. Weitz, *Mater. Today*, 2008, **11**, 18–27.
2 Ho Cheung Shum, Adam R. Abate, Daeyeon Lee, Andre R. Studart, Baoguo Wang, Chia-Hung Chen, Julian Thiele, Rhutesh K. Shah, Amber Krummel and David A. Weitz, *Macromolecular Rapid Communications*, 2010, **31**, 108–118.
3 Fude Cui, Dongmei Cun, Anjin Tao, Mingshi Yang, Kai Shi, Min Zhao and Ying Guan, *J. Controlled Release*, 2005, **107**, 310–319.
4 Myung-Han Lee, Seong-Geun Oh, Sei-Ki Moon and Seong-Youl Baey, *J. Colloid Interface Sci.*, 2001, **240**, 83–89.
5 V. Muguet, M. Seiller, G. Barratt, O. Ozer, J. P. Marty and J. L. Grossiord, *J. Controlled Release*, 2001, **70**, 37–49.
6 Chia-Hung Chen, Rhutesh K. Shah, Adam R. Abate and David A. Weitz, *Langmuir*, 2009, **25**, 4320–4323.
7 Zhihong Nie, Wei Li, Minseok Seo, Shengqing Xu and Eugenia Kumacheva, *J. Am. Chem. Soc.*, 2006, **128**, 9408–9412.
8 T. G. Mason and J. Bibette, *Phys. Rev. Lett.*, 1996, **77**, 3481–3484.
9 C. Goubault, K. Pays, D. Olea, P. Gorria, J. Bibette, V. Schmitt and F. Leal-Calderon, *Langmuir*, 2001, **17**, 5184–5188.
10 A. S. Utada, E. Lorenceau, D. R. Link, P. D. Kaplan, H. A. Stone and D. A. Weitz, *Science*, 2005, **308**, 537–541.
11 Shingo Okushima, Takasi Nisisako, Toru Torii and Toshiro Higuchi, *Langmuir*, 2004, **20**, 9905–9908.
12 Takasi Nisisako and T. Torii, *Lab Chip*, 2008, **8**, 287–293.
13 T. Nisisako, T. Torii, T. Takahashi and Y. Takizawa, *Adv. Mater.*, 2006, **18**, 1152–1156.
14 Georgios Tetradis-Meris, Damiano Rossetti, Concepcion Pulido de Torres, Rong Cao, Guoping Lian and Ruth Janes, *Ind. Eng. Chem. Res.*, 2009, **48**, 8881–8889.
15 Wei Li, Jesse Greener, Dan Voicu and Eugenia Kumacheva, *Lab Chip*, 2009, **9**, 2715–2721.
16 Adam R. Abate, Julian Thiele and David A. Weitz, *Lab Chip*, 2011, **11**, 253–258.
17 Assaf Rotem, Adam R. Abate, Andy S. Utada, Volkert van Steijn, David A. Weitz, unpublished work.
18 Henrik Bruus, *Theoretical Microfluidics*, Oxford University Press, Oxford, 2008, p. 51.
19 J. Cooper McDonald, David C. Duffy, Janelle R. Anderson, Daniel T. Chiu, Hongkai Wu, Olivier J. A. Schueller and George M. Whitesides, *Electrophoresis*, 2000, **21**, 27–40.
20 Janelle R. Anderson, Daniel T. Chiu, Rebecca J. Jackman, Oksana Cherniavskaya, J. Cooper McDonald, Hongkai Wu, Sue H. Whitesides and George M. Whitesides, *Anal. Chem.*, 2000, **72**, 3158–3164.
21 Julian Thiele, Maike Windbergs, Adam R. Abate, Martin Trebbin, Ho Cheung Shum, Stephan Forster and David A. Weitz, *Lab Chip*, 2011, **11**, 2362–2368.